Volume 7, Issue 3, July 2020 ISSN: 2348-8565 (Online)

International Journal of Modern Engineering and Research Technology

Website: http://www.ijmert.org Email: editor.ijmert@gmail.com

Annealing Temperature Influenced Structural, Electrical and Optical Properties of DC Magnetron Sputtered Cr_2O_3 Thin Films

Gopal Naik B
Research Scholar
Department of Physics,
Sri Venkateswara University,
Tirupati (A.P.), India
E-mail: gopalnaik.sri@gmail.com

Uthanna S
Assistant *Professor*
Department of Physics,
Sri Venkateswara University,
Tirupati (A.P.), India
E-mail: uthanna@rediffmail.co

ABSTRACT

Thin films of chromium oxide were deposited on to glass and silicon substrates held at room temperature by DC reactive magnetron sputtering of chromium target at different oxygen partial pressures. The films formed at oxygen partial pressure of 4×10^{-4}Torr were of Cr_2O_3 films. These films were annealed at different temperatures in the range 300–550°C and studied the effect of annealing temperature on the chemical binding configuration, structure, electrical and optical properties. The as-deposited and the films annealed at temperature of 400°C were amorphous in nature. The films annealed at temperatures 450°C and above were of polycrystalline with rhombohedral Cr_2O_3 with enhanced in the crystallinity. Fourier transform infrared spectroscopic studied exhibited the characteristic vibration modes of Cr_2O_3. The electrical resistivity of the films increased from 14.0 Ωcm to 22.8 Ωcm and optical band gap increased from 3.18 eV to 3.27 eV with increase of annealing temperature from 300°C to 550°C.

Keywords:— *Chromium oxide thin films, Structure, XPS, FTIR, Optical properties, DC magnetron sputtering.*

I. INTRODUCTION

Chromium is a transition metal which exhibit nine oxidation states. These oxides of chromium form by varied stoichiometry depending on the method of preparation and process conditions fixed for the growth in the thin film form.

Among these oxides, chromium oxide (Cr_2O_3) is thermally stable and hardest oxide state of chromium providing good wear and corrosion resistance and low coefficient of friction [1]. Cr_2O_3 thin films find potential applications such read-write heads in digital magnetic recording devices [2], lubricant coatings for gas bearings [3], absorber layer in solar cells [4], shields in flexible solar cells [5] and anode for lithium ion batteries [6]. It also find applications in sensing of ethanol, chlorine and hydrogen sulfide gases [7] and catalyst for various photochemical and environment applications [8]. Different thin film deposition methods such as vacuum evaporation [9, 10], electron beam evaporation [11], pulsed laser deposition [12, 13], DC magnetron sputtering [14-18], RF magnetron sputtering [19-21], cathodic arc deposition [22, 23], and chemical routes namely spray pyrolysis [24, 25], sol-gel process [26, 27], atomic layer deposition [28], electro-deposition [29] and chemical

vapour deposition [30]. Among these methods, DC reactive magnetron sputtering received much attention because of deposition of films by sputtering of metallic chromium target in presence of reactive gas of oxygen and sputter gas of argon. The physical properties of sputter deposited films depend on the sputter process parameters namely oxygen partial pressure, substrate temperature, bias applied to the substrate and sputter power. In this investigation, thin films of Cr_2O_3 were deposited on to glass and silicon substrates held at room temperature by DC reactive magnetron sputtering of metallic chromium target at different oxygen partial pressures. The as-deposited films were also annealing in air at different temperatures in the range from 300°C to 550°C and studied their chemical binding configuration, crystallographic structure and surface morphology, electrical and optical properties.

II. Experimental

Chromium oxide thin films were deposited onto glass and p- silicon substrates held at room temperature by DC magnetron sputtering method using Hind Hivac coating unit. The box type sputter chamber was evacuated by diffusion pump and direct drive rotary pump combination to achieve the ultimate pressure of 5×10^{-6} Torr. Chromium target (99.99% pure) with 50 mm diameter and 3 mm thickness was used as sputter target. Oxygen gas was admitted into the sputter chamber through fine controlled needle valve. After attaining the required oxygen partial pressure, argon gas was admitted to the sputter chamber to a pressure of 1×10^{-2} Torr. In order to achieve equal thickness, the films were deposited at different oxygen partial pressures with different times of duration. Deposition conditions maintained for preparation of chromium oxide films are given in table 1.

Table 1. Conditions for deposition of Cr_2O_3 films by DC magnetron sputtering

Deposition method	DC Magnetron sputtering
Sputter target	Chromium (50 mm diameter)
Target - substrate distance	70 mm
Substrates	Glass and p- Silicon (100)
Substrate temperature	30°C
Sputter power	70 Watt
Ultimate pressure	5×10^{-6} Torr
Oxygen partial pressure	5×10^{-5} - 6×10^{-4} Torr
Sputter pressure	1×10^{-2} Torr

The deposited films were characterized for chemical composition using energy dispersive X-ray analyzer (Oxford Instruments Inca Penta FETX3) attached to the scanning electron microscope (Carl Zeiss model EVO MAIS). Chemical binding configuration and core level binding energies of the films was determined from X-ray photoelectron spectroscope (Physical Electronics Model PHI 5700). Fourier transform infrared spectroscopic studies was performed with Fourier transform infrared spectrophoto-meter (Thermo-Nicolet model 6700). Surface morphology of the films formed on silicon substrates was studied with field emission scanning electron microscope (Hitachi model S-4100). X-ray diffractometer (X'pert Pro PAN Analytical) with Cu K_α radiation (wavelength of 0.15406 nm) was used to determine the crystallographic structure and crystallite size of the films. Electrical resistivity of the films was measured using van der Pauw method. Optical transmittance of the films formed on glass substrates was recorded using JASCO spectrophotometer (model V570) UV-Vis-NIR double beam spectrophotometer in the wavelength range 300 - 1400 nm in order to determine the optical band gap and refractive index.

III. Results and Discussion

The thickness of the deposited films was determined with Dektak depth profilometer was in the range 220–240 nm. The deposition rate of the films was calculated from the thickness of the film and duration of deposition. Deposition rate of the films depend on the oxygen partial pressure prevailed the sputter chamber. Variation of deposition rate of Cr_2O_3 films on the oxygen partial pressure is given in figure 1. The deposition rate of the films formed at low oxygen partial pressure of 5×10^{-5} Torr was 12.2 nm/min. As the oxygen partial pressure increased to 6×10^{-4} Torr the deposition rate decreased to 7.2 nm/min. The decrease in the deposition rate with increase of oxygen partial pressure was due to decrease in the sputter yield of the sputter species due to reaction of oxygen and form chromium oxide. Such a reduction in the deposition rate with the oxygen partial pressure was also noticed by Mohammadtaheri et. al. [31] in the reactive magnetron sputtered Cr_2O_3 films. Barshilia and Rajam [17] reported that the Cr_2O_3 films formed by pulsed DC magnetron sputtering, the deposition rate decreased from 33 nm/min to 13 nm/min. with increase of oxygen flow rate from 7 sccm to 15 sccm respectively.

Chemical composition of the deposited Cr_2O_3 films was determined by energy dispersive X-ray analysis. Figure 2 shows the energy dispersive X-ray analyses spectra of Cr_2O_3 films formed on silicon substrates and at different oxygen partial pressures. It is seen that the characteristic chromium and oxygen kinetic energy peaks along with silicon. The silicon signal arises from the silicon substrate. The intensity of oxygen peak increased with increase of oxygen partial pressure.

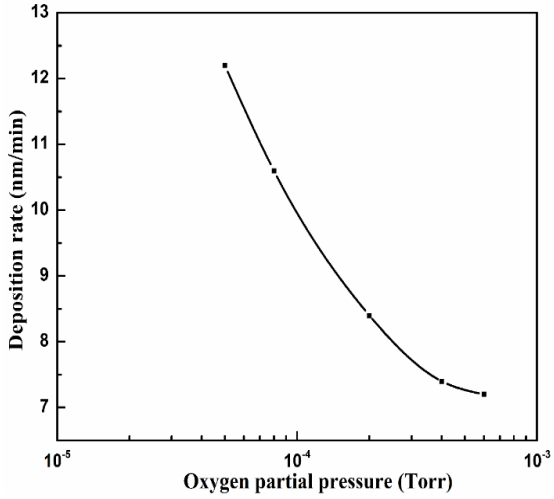

Figure 1. Dependence of deposition rate on the oxygen partial pressure of Cr_2O_3 films.

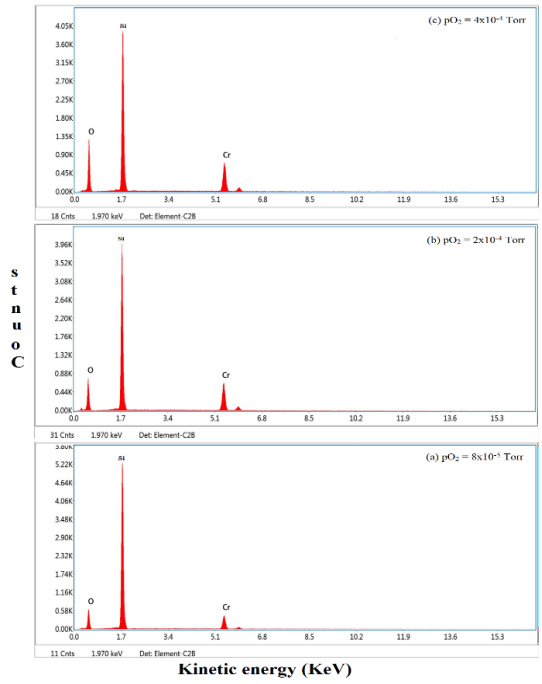

Figure 2. EDAX spectra of Cr_2O_3 films formed at different oxygen partial pressures.

Chemical composition of the films was determined from the characteristic peaks of chromium and oxygen by considering their sensitively factors. Table 2 shows the chemical composition of the Cr_2O_3 films deposited at different oxygen partial pressures. The films formed at low oxygen partial pressure of 5×10^{-5} Torr were of mixed phase of chromium and chromium oxide hence of excess chromium. The films deposited at 4×10^{-4} Torr and above were of

single phase Cr_2O_3 due to the presence of required oxygen in the sputter chamber to react with chromium and form chromium oxide films. It indicated that oxygen partial pressure of 4×10^{-4} Torr is an optimum to deposit Cr_2O_3 films by DC reactive magnetron sputtering.

Table 2. Chemical composition of Cr_2O_3 films determined with EDAX.

Oxygen partial pressure	Chemical composition (at. %)	
	Chromium (at. %)	Oxygen (at. %)
8×10^{-5}Torr	46.2	53.8
2×10^{-4}Torr	41.9	58.1
4×10^{-4}Torr	40.2	59.8

X-ray photoelectron spectroscopic studies

The chemical binding configuration and core level binding energies of the constituent elements present in the films was analyzed with X-ray photoelectron spectroscope. Figure 3a shows the XPS survey scan spectra of Cr_2O_3 films formed at different oxygen partial pressures. It is seen from the spectra that the films contained the characteristic core level binding energy peaks of chromium and oxygen. The core level binding energies observed at about 575 eV and 586 eV correspond to the chromium Cr $2p_{3/2}$ and Cr $2p_{1/2}$ due to spin-orbit splitting in the energy levels of Cr 2p. The peak located at about 530 eV was related to the core level binding energy of oxygen O 1s. Figure 3b and 3c shows the XPS narrow scan spectra at core level binding energies of chromium Cr 2p and oxygen O 1s of Cr_2O_3 films formed at different oxygen partial pressures. The films deposited at oxygen partial pressure of $2x10^{-4}$ Torr consisted of core level binding energies of 574.6 eV and 584.0 eV related to Cr $2p_{3/2}$ and Cr $2p_{1/2}$ respectively with spin-orbit splitting energy separation of 9.4 eV correspond to the elemental chromium. Along with this, the core level binding energies located at 576.6 eV and 586.3 eV were of Cr $2p_{3/2}$ and Cr $2p_{1/2}$ energy separation of 9.7 eV related to Cr_2O_3. It revealed that films formed at $2x10^{-4}$ Torr were of mixed phase of chromium and Cr_2O_3. The films deposited at oxygen partial pressure of 4×10^{-4} Torr showed core level binding energies at 576.6 eV and 586.3 eV related to chromium Cr $2p_{3/2}$ and Cr $2p_{1/2}$ with spin-orbit spitting energy separation of 9.7 eV correspond to single phase Cr_2O_3. From these studies it confirms that the films deposited at oxygen partial pressure of 4×10^{-4} Torr were single phase Cr_2O_3. Barshilia and Rajam [3] reported that the core levels of 577.1 eV and 586.9 eV related to Cr $2p_{3/2}$ and Cr $2p_{1/2}$ with spin-orbit spitting energy separation of 9.8 eV in Cr_2O_3 films, and the binding energies of 574.3 eV and 584.1 eV of Cr $2p_{3/2}$ and Cr $2p_{1/2}$ with separation in the energy of 9.2 eV in chromium films formed by magnetron sputtering. It is to mention here that core level binding energy of Cr $2p_{1/2}$ located at 578.8 eV, 576.3 eV and 576.8 eV were CrO_3, CrO_2 and Cr_2O_3 respectively [5]. The Cr_2O_3 films deposited at optimum oxygen partial pressure of 4×10^{-4} Torr were also annealed in air at different temperatures in the range from 300°C to 550°C and studied its influence on the structure, electrical and optical properties.

Fourier transform infrared studies

Chemical bonding configuration of the Cr_2O_3 films formed on silicon substrates was analyzed with the Fourier transform infrared spectroscope. Figure 4 depicts the Fourier transform infrared transmittance spectra of Cr_2O_3 films annealed at different temperatures. The as-deposited films were not shown any absorption bands due to the amorphous nature.

Films annealed at 450°C consisted of absorption bands at 535 cm^{-1}, 610 cm^{-1} and 730 cm^{-1}. The absorption band located at

535 cm^{-1} was due to the symmetric stretching vibration mode of Cr-O [32]. The band located at 610 cm^{-1} was due to anti symmetric vibration of Cr-O and 730 cm^{-1} the characteristic vibration modes of Cr - O in Cr_2O_3 [33,34].

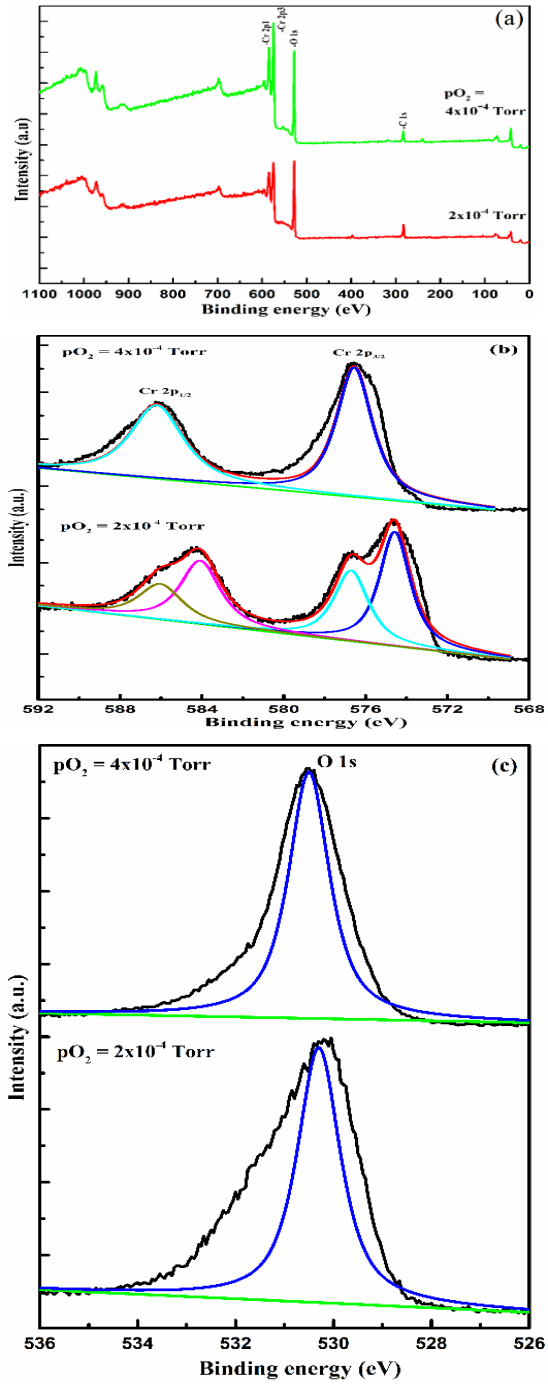

Figure 3. XPS (a) survey scan, and narrow scan spectra of (b) chromium Cr 2p and (c) oxygen O 1s of Cr_2O_3 films formed at different oxygen partial pressures.

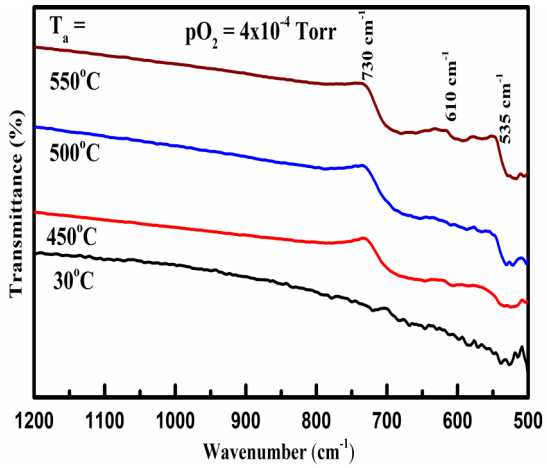

Figure 4. Fourier transform infrared transmittance spectra of Cr_2O_3 films annealed at different temperatures.

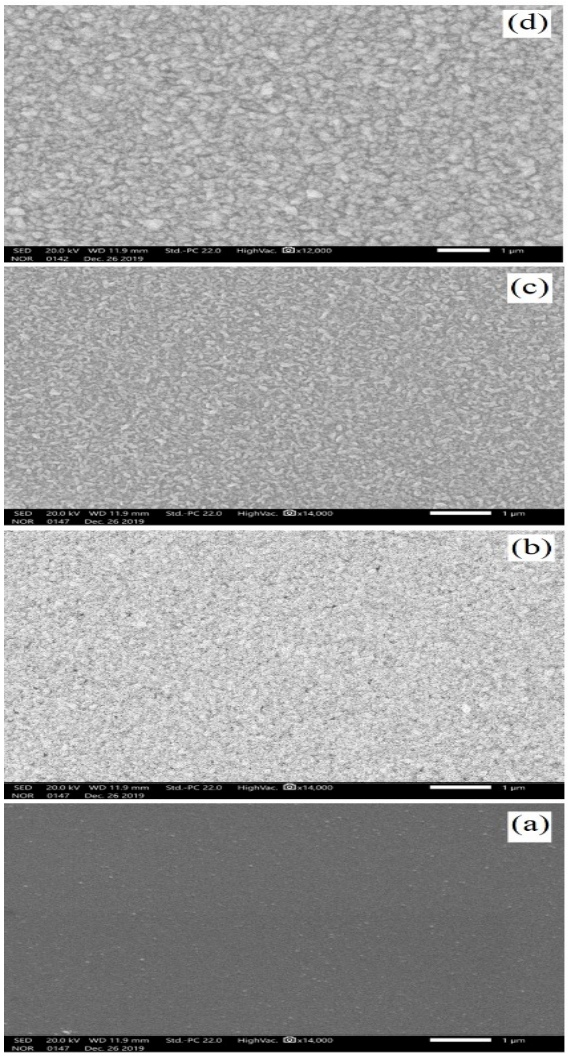

Figure 5. Scanning electron micrographs of (a) as-deposited, and the films annealed at (b) 450°C, (c) 500°C and (d) 550°C.

Surface morphology

Surface morphology of the films was analyzed with scanning electron microscope. Figure 5 shows the scanning electron micrographs of Cr_2O_3 films annealed at different temperature. The as-deposited films were of smooth surface. As the annealing temperature increased 450°C the size of the grain increased and the grains were uniformly distributed in the films. The grain size of the as-deposited films was 20 nm. When the annealing temperature increased from 450°C to 550°C the grain size increased from 42 nm to 65 nm respectively. As the annealing temperature increased the given thermal energy activate the growth of larger size grains.

X-ray diffraction studies

Figure 6 shows the XRD profiles of as-deposited and the Cr_2O_3 films annealed at different temperatures. The as-deposited and the films annealed at 400°C were not shown any diffraction peak which indicated the amorphous nature. The films annealed at temperature of 450°C showed weak diffraction peaks at 2θ values of 34.33°, 36.98°, 51.09° and 55.96° related to (104), (110), (113) and (116) indicated the polycrystalline nature with rhombohedral phase of Cr_2O_3. It is in accordance with the JCPDS card No. 38-1479 of Cr_2O_3. As the annealing temperature increased to 500°C, the intensity of the reflections enhanced due to improvement in crystallinity of the films. Addition reflections of (012), (024) and (214) and (300) were present along with (104), (110), (113) and (116) and the intensity of peaks enhance with increase of annealing temperature from 500°C and 550° C. It is to be noted that amorphous Cr_2O_3 films were achieved by Dwivedi and Biswas in pulsed laser deposited [12] and Lin and Sproul in DC magnetron sputtered films [14]. Khojier et al. noticed a mixed phase of Cr_3O and Cr_2O_3 at temperature of 400°C whereas single phase Cr_2O_3 films at 500°C in RF magnetron sputtering [19]. He et al. reported that the amorphous to polycrystalline phase transformation at temperature of 450°C in cathodic arc deposited Cr_2O_3 films [22]. Sim et al. [23] achieved rhombohedral structured Cr_2O_3 films by cathodic are deposition after annealing at temperature of 600°C. The crystallite size of the films (D) was calculated from the X-ray diffraction peaks using the Debye – Scherrer's relation [35],

$$D = 0.9\lambda/\beta\cos\theta \quad \text{..... (1)}$$

where λ is the wavelength of copper X-ray radiation, β the full width at half maximum intensity of X-ray diffraction peak and θ the diffraction angle. The crystallite size of the films increased from 37 nm to 63 nm with increase of annealing temperature from 450°C to 550°C due to improvement in the crystallinity. Dislocation density (δ) and strain (ε) developed in the films were calculated from the X-ray diffraction peaks employing the relations,

$$\delta = 1/D^2 \quad \text{..... (2)}$$

and

$$\varepsilon = \beta\cos\theta/ \quad \text{..... (3)}$$

Dislocation density of the films decreased from 7.3×10^{15} lines/m^2 to 2.4×10^{15} lines/m^2 with increase of annealing temperature from 450°C to 550°C respectively. Stain developed in the films also decreased from 3.1×10^{-3} to 1.9×10^{-3} with increase of annealing temperature from 450°C to 550° C. The decrease in the dislocation density and strain with increase of annealing temperature was mainly due to improvement in the crystallinity of the films.

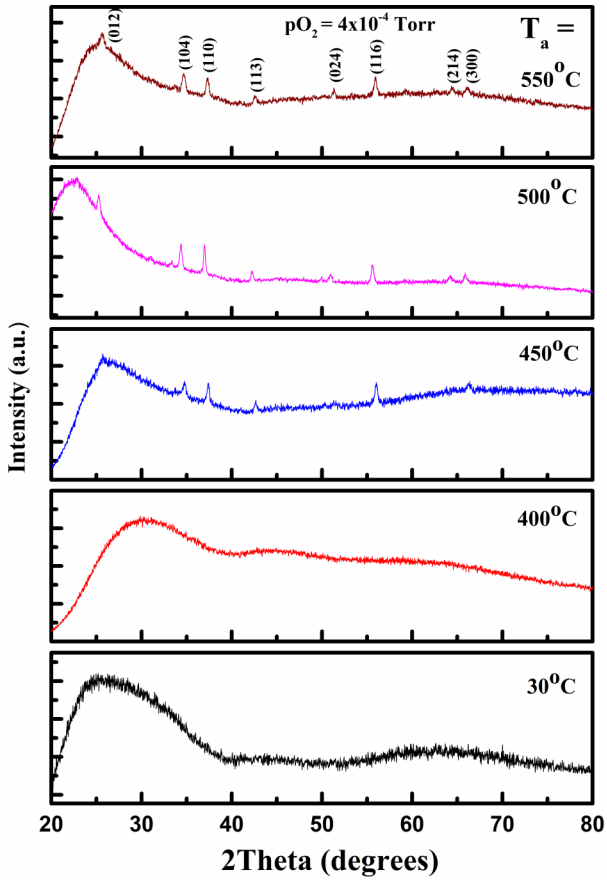

Figure 6. X-ray diffraction profiles of Cr_2O_3 films annealed at different temperatures

Electrical properties

The dependence of electrical resistivity on annealing temperature of Cr_2O_3films is shown in figure 7. The electrical resistivity of the as-deposited films was 6.3 Ωcm. The resistivity of the films increased from 14.0 Ωcm to 22.8 Ωcm with increase of annealing temperature from 300°C to 550°C respectively. The enhancement in the resistivity with annealing temperature was due decrease in the oxygen ion vacancies and improvement in the crystallinity. Wang et al. [36] reported the electrical resistivity of 10 Ωcm by RF magnetron sputtering and Dwivedi and Biswas [12] 0.1 Ωcm in pulsed laser deposited Cr_2O_3 films. Huang et al. [15] reported the high electrical resistivity of 3×10^5Ωcm in cathodic arc deposited films and it decreased with increase of bias voltage during the deposition of the films.

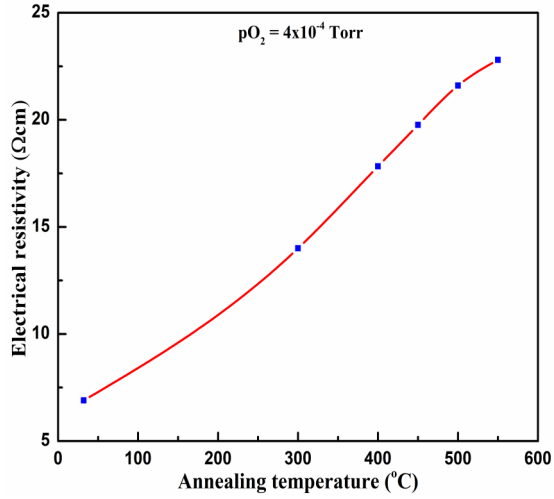

Figure 7. Dependence of electrical resistivity of Cr_2O_3 films on annealing temperature.

Optical properties

Optical transmittance of the films formed on glass substrates was recorded in the wavelength range 300 – 1400 nm in order to study the optical absorption and to determine the optical band gap and refractive index. Figure 8 shows the optical transmittance spectra of Cr_2O_3 films annealed at different temperatures. Optical transmittance of the films was influenced by the annealing temperature. The transmittance of the films increased with increase of annealing temperature. The increase of transmittance was due to decrease in the oxygen ion vacancies along with improved crystallinity. The fundamental optical absorption edge of the films shifted towards lower wavelengths side. The optical absorption coefficient (α) of the films was determine from the optical transmittance (T) data and thickness (t) using the relation

$$A = -(1/t)\ln(T) \quad \ldots\ldots\ldots\ldots\ldots\ldots\ldots (4)$$

In order to determine the optical band gap, the optical absorption data of the films was fitted to the Tauc's relation [37]

$$(\alpha h\nu)^2 = A(h\nu - Eg) \quad \ldots\ldots\ldots\ldots\ldots\ldots\ldots (5)$$

Where hν is the photon energy, Eg the optical band gap and A absorption edge width parameter. Figure 9 shows the plots of $(\alpha h\nu)^2$ versus photon energy of the films annealed at different temperatures. The optical band gap of as-deposited Cr2O3 film was 3.15 eV. The band gap increased from 3.20 eV to 3.27 eV with increase of annealing temperature from 450°C to 550° C. From the optical transmittance

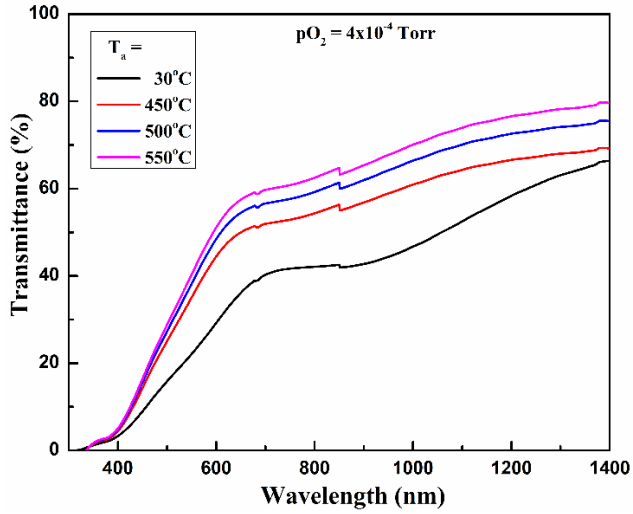

Figure 8. Optical transmittance spectra of Cr_2O_3 films annealed at different temperatures.

interference, the refractive index (n) of the films was calculated using Swanepoel envelope method [38] using the relation

$$n(\lambda) = [N+ (N^2-s^2)^{1/2}]^{1/2} \ldots\ldots\ldots\ldots (6)$$

with

$$N(\lambda) = 2s[T_M-T_m)/(T_M-T_m)]+(s^2+1)^{1/2} \ldots (7)$$

where n(λ) is the refractive index of film at wavelength λ, T_M and T_m the transmittance maxima and minima respectively and s the refractive index of the substrate. Wavelength dependence refractive index of Cr_2O_3 films annealed at different temperatures is shown in figure 10. The refractive index of the films formed at 30°C was low and increased with increase of annealing temperature. The refractive index decreased with increase of wavelength and remains almost constant at higher wavelengths. At a fixed wavelength (λ = 500 nm) the refractive index of the as-deposited Cr_2O_3 films was 2.00. The refractive index of the films increased from 2.04 to 2.08 with increase of annealing temperature from 450°C to 550°C. Barshilia and Rajam [17] reported refractive index of 2.15 in DC reactive magnetron sputtered Cr_2O_3 films. Julkarnian et al. [9] obtained the refractive index of 1.45 in the films formed at room temperature and increased to 1.60 after annealing at 300°C. Ivanova et al. [30] noticed the refractive index of 2.2 in chemical vapour deposited Cr_2O_3 films.

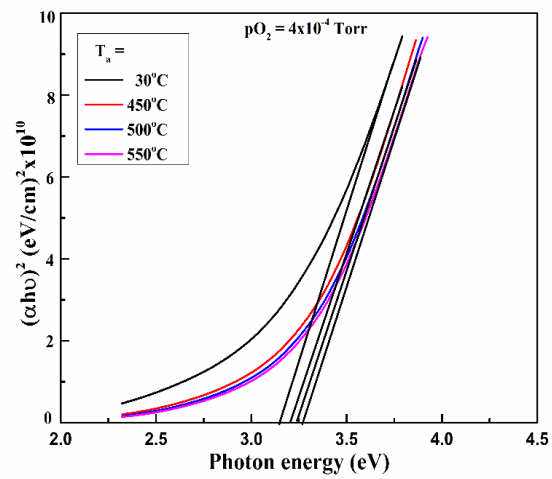

Figure 9. plots of $(\alpha h\nu)^2$ versus photon energy of Cr_2O_3 films annealed at different temperatures.

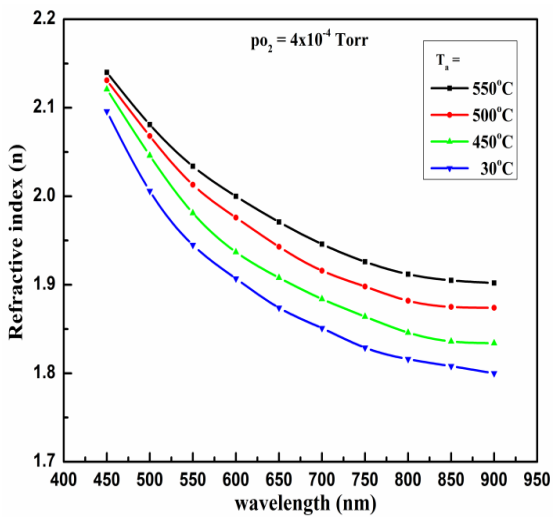

Figure 10. Refractive index of Cr_2O_3 films annealed at different temperatures.

IV. CONCLUSION

Chromium oxide films were formed on glass and p-type silicon substrates using DC reactive magnetron sputtering at different oxygen partial pressures. The films deposited at oxygen partial pressure of 4×10^{-4} Torr were of stoichiometric Cr_2O_3. These Cr_2O_3 films were annealed at different temperatures. Influence of annealing temperature on the chemical binding configuration and crystallographic structure, electrical and optical properties was studied. The as-deposited and the films annealed upto 400°C were amorphous in nature. As the temperature increased to 450°C and above were of polycrystalline with rhombohedral structured Cr_2O_3. The crystallite size of the films increased from 37 nm to 63 nm with increase of annealing temperature from 450°C to 550°C respectively. The electrical resistivity of the films increased from 14.0 Ωcm to 22.8 Ωcm and optical band gap increased from 3.20 eV to 3.27 eV with increase of annealing temperature from 450°C to 550°C.

ACKNOWLEDGEMENT

One of the authors, Prof. S. Uthanna is thankful to the University Grants Commission, New Delhi for the award of UGC-BSR Faculty Fellowship.

REFERENCES:

[1] G.S.A.M. Theunissen, Wear coating for magnetic thin film magnetic recording heads, Tribol. Int., 31 (1998) 519.

[2] E. Sourty, L. Sullivan, M.D. Bijker, chromium oxide coatings applied to magnetic tape heads for improved wear resistance, Tribol. Int., 36 (2003) 389.

[3] N. He, H. Li, L. Ji, X. Liu, H. Zhou and J. Chen, Reusable chromium oxide coating with lubricating behavior from 25°C to 100°C due to a self-assembled mask-like surface structure, Surf. Coat. Technol., 321 (2017) 300.

[4] P. Qin, G. Fang, Q. Zhang, F. Chen, J. Van, X. Zhao, N. Sun and X. Fan, Organic solar cells with p-type amorphous Cr_2O_3 film as hole-transport layer, Thin Solid Films, 512 (2011) 4334.

[5] M. Kaltenbrunner, G. Adem, E.D. Glowacki, M. Drack, R. Schwodiauer, L. Leonat, D.H. Apaydin, H. Groiss, M.C. Scharber, M.S. White, N.S. Sariciftci and S. Bauer, Flexible high power per weight perovskite solar cells with chromium oxide-metal contact for improved stability in air, Nat. Mater., 4 (2015) 1032.

[6] J.T. Li, V. Maurice, J.S. Mzowiecka, A. Seyeux, S. Zanna, L. Klein, S.G. Sun and P. Marcus, XPS, time of flight, SIMS and polarization modulation IRRAS studies of Cr_2O_3 thin film as anode for lithium ion battery, Electrochem. Acta, 54 (2009) 3700.

[7] V. Balouria, A. Kumar, A. Singh, S. Samatha, A.K. Debnath, A. Mahajan, B.K. Bedi, D.K. Aswal, S.K. Gupta and J.V. Yakmi, Temperature dependent H_2S and Cl_2 sensing selectivity of Cr_2O_3 thin films, Sens. Actuat., B 157 (2011) 466.

[8] C.M. Pordier, F. Rodrigues, P. Marcus, M.V. Landau, M.L. Kaliya, A. Gutman and H.M. Herskowitz, Supported chromia catalyst for oxidation of organic compounds: The state of chromium phase and catalytic performance, Appl. Cat., B 27 (2000) 73.

[9] M. Julkarnain, J. Hussain, K.S. Sharif and K.A. Khan, Optical properties of thermally evaporated Cr_2O_3 thin films, Can. J. Chem. Eng. Technol., 3 (2012) 81.

[10] A. Kadari, T. Schemme, D. Kadri and J. Wollschlager, XPS and morphological properties of Cr_2O_3 thin films grown by thermal evaporation method, Results in Phys., 7 (2017) 3124.

[11] M.F. Al-Kuhaili and S.M.A. Durrani, Optical properties chromium oxide thin films deposited by electron beam evaporation, Optical Mater., 29 (2007) 709.

[12] S. Dwivedi and S. Biswas, Enhanced magneto-resistance in pulsed laser deposited stable chromium oxide thin films, Thin Solid Films, 655 (2018) 13.

[13] D.K. Panda, A. Singh, R. Divakar, N. Gopala Krishna, V.R. Reddy, R. Thirumurugesan, S. Murugesan, P. Parameswaran and E. Mohandas, Thin Solid Films, 660 (2018) 328.

[14] J. Lin and W.D. Sproul, Structure and properties of Cr_2O_3 and coatings deposited using DCMS, PDCMS and DOMS, Surf. Coat. Technol., 276 (2015) 70.

[15] K. Huang, L. Li, L. Wang, G. Dong and Y. Xu, Effect of DC bias and RF self-bias on the structure and properties of chromium oxide coatings prepared by vacuum cathodic arc deposition, Vacuum, 164 (2019) 325.

[16] D. Gall, R. Gampp, H.P. Lang and P. Oelhafen, J. Vac. Sci. Technol. A14 (1996) 374.

[17] H.C. Barshilia and K.S. Rajam, Growth and characterization of chromium oxide by pulsed direct current reactive unbalanced magnetron sputtering, Appl. Surf. Sci., 255 (2008) 2925.

[18] V. Jella, S.-H. Kang, S.V.N. Pammi, J.-H. Eom, J.-R. Jeong and S.-G. Yoon, Thermoelectric properties of nanocomposite n-type Cr_2O_3/Cr films deposited by reactive sputtering, Vacuum, 140 (2017) 71.

[19] S. Khamlich, R. McCrindle, Z.Y. Nuru, N. Cingo and M. Maaza, Annealing effect on the structural and optical properties of Cr/α-Cr_2O_3monodispersed particles based solar cells, Appl. Surf. Sci., 265 (2013) 745.

[20] X. Pang, K.W. Gao, H.S. Wang, I. Qiao, Y.B. Wang and A.A. Volinsky, Interfacial microstructure of chromium oxide coatings, Adv. Eng. Mater., 9 (2001) 594.

[21] F. Luo, X. Pang, K. Gao, H. Yang and Y. Wang, Role of deposition parameters on microstructure and mechanical properties of chromium oxide coating, Surf. Coat. Technol., 202 (2007) 58.

[22] N. He, L. Ji, X. Liu, H. Li, H. Zhou and J. Chen, Role of annealing temperature on the evolution of microstructure and properties of Cr_2O_3 films, Appl. Surf. Sci., 357 (2015) 1472.

[23] J.-K. Sim, S.-K. Lee, J.-S. Kim, K.-U. Jeong and H.-K. Ahn, Efficiency enhancement CIGS compound solar cells fabricated using homo-morphic thin Cr_2O_3 diffusion barrier formed on stainless steel substrate, Appl. Surf.

Sci., 389 (2016) 645.

[24] R.H. Misho, W.A. Murad and G.H. Fattahallah, Preparation and optical properties of thin films of CrO_3 and Cr_2O_3 prepared by the method of chemical spray deposition, Thin Solid Films, 169 (1989) 235.

[25] V.L. Ratia, D. Zhang, J.L. Daure, P.H. Shipway, D.G. McCartney and D.A. Stewart, Sliding wear of a self-mated thermally sprayed chromium oxide coating in a simulated PWR water environment, Wear, 426-427 (2019) 1466.

[26] S. Lalitha, R. Sathyamurthy, S. Senthilrasu, A. Subramanyan and K. Natarajan, Solar Energy Mater. Solar Cells, 82 (2004) 187.

[27] K. La-Rashedi, M. Farooqui and G. Rabbani, Orient J. Phys., 34 (2013) 2203.

[28] A. Tarre, J. Aarik, H. Mandar, A. Niilish, R. Purna, R. Rammula, T. Uustare, A. Rosentaland V. Sammelselg, Atomic layer deposition of Cr_2O_3 thin films: Effect of crystallization on growth and properties, Appl. Surf. Sci., 254 (2008) 5149.

[29] Q. Zhou, Z. Lu, Y. Ling, J. Wang, R. Wang, Y. Li and Z. Zhang, Characteristic and behavior of an electro-deposited chromium (III) oxide/ silicon carbide composite coating under hydrogen plasma environment, Fusion Eng. Design, 143 (2019) 137.

[30] T. Ivanova, K. Gesheva, A. Cziraki, A. Szekeres and E. Vlaikova, Structural transformation and their relation to the optoelectronic properties of chromium oxide thin films, J. Phys: Conf. Series, 113 (2008) 012030.

[31] M. Mohammadtaheri, Q. Yang, Y. Li and J. Corona-Gomez, Effect of deposition parameters on the structure and mechanical properties of chromium oxide by reactive magnetron sputtering, Coatings, 8 (2018) 111.

[32] C. Madi, M. Tabbal, T. Christidis, S. Isber, B. Nsouli and K. Zahraman, Microstructural characterization of chromium oxide thin films grown by remote plasma assisted pulsed laser deposition, J. Phys.: Conf. Series, 59 (2007) 600.

[33] Y. Jing, L.F. Ray and N. Wayde, Transition of chromium oxide particles to chromium oxide: Hot stage Raman spectroscopic study, J. Raman. Spectros., 42 (2010) 1142.

[34] S. Dwivedi, J. Jadhav, H. Sharma and S. Biswas, Pulsed laser deposited ferromagnetic chromium dioxide thin films for applications in spintronics, Phys. Procedia, 54 (2014) 62.

[35] B.D. Cullity, S.R. Stock, Elements of X-ray diffraction, Printice Hall, Englewood Cliffs, NJ (2001) 170.

[36] F. Wang, Y. Abe, M. Kuwamura, K.H. Kim T. Kiba, Surf. Coat. Technol., 387 (2020) 25509.

[37] J. Tauc, Amorphous and Liquid Semicon-ductor, Plenum Press, NY (1974).

[38] R. Swanepoel, Determination of film thickness and optical constant of amorphous silicon, J. Phys. E 16 (1983) 1216.